Universitatea Naţională de Ştiinţă şi Tehnologie POLITEHNICA Bucureşti

DOCTORAL SCHOOL OF ELECTRICAL ENGINEERING

SUMMARY OF THE DOCTORAL THESIS

Research on the influence of external factors on some polymeric substances

PhD student: Eng. Costel Păun
Scientific Coordinator: Prof.dr.ing. Laurenţiu Marius Dumitran

BUCUREŞTI 2024

Cuprins

Introduction

In the last century and a half, the discovery and production of polymeric materials has led to the expansion of the range of activities in many sectors of activity and has successfully contributed to the replacement of traditional materials. The most important groups of polymeric materials are plastics, followed by fibers and elastomers. Polymeric materials are the basis of important industrial products. The rapid increase in their production is due to both social factors and the need to replace classic materials. Polymer science is a relatively new discipline that deals with natural plastics, synthetic fibers, adhesives, paints, sealants, rubbers, lubricants, materials used for coatings, degradable sutures, etc., used in a wide range of technical applications, medical applications, etc.

From an economic and application point of view, plastic materials are divided into goods characterized by low cost and high volume such as (polyvinyl chloride, polyethylene, polypropylene, etc.) and engineering materials characterized by higher cost and low volume (polycarbonate, polyimide, etc.). Natural, artificial (derived from natural organic raw materials) and synthetic fibers (derived from synthetic organic raw materials) have characteristics depending on the application where they are used (high aspect ratio, special mechanical characteristics, etc.). Elastomers have the property of stretching and returning to their original shape in a short time [1-3].

The purpose of this research was to study the effect of certain external factors on polymeric materials used in various technical applications, in order to determine the risk factors, the preventive measures that must be taken to eliminate the influences of these factors, and to serve as a starting point for future research to design new materials more resistant to various external factors.

PART I
General notions about polymeric materials and their degradation under the influence of external factors
Chapter 1
General notions about polymeric materials

1.1. Brief history of plastic materials

This chapter presents a brief history of plastic materials used in various fields of activity, as well as information about their production worldwide, depending on their type and field of use.

The first plastic material was based on nitrocellulose and was obtained by Parkes in 1862 and Hyatt in 1866. By adding camphor to nitrocellulose, the first thermoplastic is obtained under the name of celluloid, which around 1900 constitutes the material used in the production of cinematographic film.

In 1907 Baekeland obtained the first heat-resistant synthetic polymer by polycondensation of phenol with formaldehyde (PF). It was produced in 1909-1910 under the trade name of Bakelite and is considered the beginning of the synthetic plastic industry.

Vinyl chloride (CV) is discovered by Regnault and Liebeg in 1835. In 1878 Baumann investigates the effect of sunlight on CV, in 1912-1916 Klatte substantiates the photopolymerization of vinyl chloride. In 1926 Ostramislenski patents a flexible film obtained from polyvinyl chloride (PVC) and a plasticizer.

In 1933 Gibson and Fawcett discovered polyethylene (PE) by the process of ethylene polymerization at high pressure. PE was successfully used by Britain to insulate electrical cables in radar installations during World War II.

Polymethyl methacrylate (PMMA) was discovered in the early 1930s by Hill and Crawford under the trade name Perspex. At the same time in Germany, the chemist and industrialist Röhm produce PMMA under the commercial name of Plexiglas. Perpex and Plexiglas entered commercial production around the same time.

In 1938, Plunkett made the synthesis of polytetrafluoroethylene (PTFE), constituting an important moment in materials science. The new polymer could not be made by melting. In order to make an easy-to-process fluoropolymer, fluorinated ethylene-propylene copolymer (FEP) was obtained, which can be processed by melting in an extruder.

Saturated polyesters (PES) were studied in 1929 by Carothers and Whinfield and Dickson (1941–1946). The most important polymer in this group is polyethylene terephthalate (PET), first produced in 1955 and used as a plastic, film and fiber.

The Bayer company manufactured polyurethanes (PU) in 1937 as a response to Carothers' research on polyamides. In 1950, flexible foams are obtained from polyesters and PU for the production of plastics (1961), corrosion-resistant fibers, coatings, elastomers, foams.

Thermosetting polyimide (PI) resins appeared after 1953 and became commercially available in 1963.

Polysulfone appears around 1965. Polyarylsulfones are commercially available from 1967-1976 and polyethersulfone in 1972. Polysulfones are transparent, light-yellow polymers. They have high temperatures of thermal distortion that are exceeded only by aramids, polyamides and polyamides.

After 1980 there is continuous growth with the development of high-performance polymers that could compete with traditional materials, such as polyamide 4-6 (1987), styrene-ethylene copolymer and syndiotactic PP in 1992 [1], [3].

Chapter 2
General notions about the degradation of polymeric materials

This chapter presents the main factors that lead to the degradation of polymeric materials, the degradation process and its consequences on the properties of polymeric materials.

The properties of polymeric materials used in different technical applications are influenced by the degradation processes during exploitation. The quality and structure of polymeric materials as well as the intensity of external stresses during exploitation determine the speed of their degradation.

These factors lead to the occurrence of depolymerization reactions, breaking of polymer chains, crosslinking reactions, oxidation reactions, hydrolysis, biodegradation, etc. Thus, products are formed that have shorter macromolecular chains, with different properties compared to the non-degraded polymer or new groups that can change the stability of the polymer.

Degradation of polymers can be induced by thermal activation, oxidation, photolysis, radiolysis or hydrolysis and if the degradation is affected by the biological environment, it can also be called biodegradation

Polymers, especially plastic materials, are subject to degradation already during the manufacturing process, during use in different environments, as well as during recycling. The rate of degradation of polymers can take decades in the case of biodegradation or a few hours during industrial processing. Degradation of polymeric materials under the action of external factors can make them unusable [22-24].

Part II
Original contributions and results
Chapter 3
Experimental methods of accelerated degradation and techniques used in the analysis of the studied polymeric materials

This chapter presents the methods of accelerated degradation (in the laboratory) of the studied polymeric materials as well as the analytical techniques used in the characterization of samples of degraded and undegraded polymeric materials.

3.1. Means of degradation

3.1.2. Degradation of polymeric materials with gamma radiation

The exposure of the studied polymer samples was carried out in a gamma ray irradiation machine (Ob-Servo Sanguis, Hungary) with a ^{60}Co source. The sample irradiation rate was 0.6 kGy/h. Irradiation was performed at room temperature [30].

3.1.3. Degradation of polymeric materials subjected to temperature cycles

The studied polymer samples were subjected to accelerated thermal aging in an ACS-CH 250 TVT climate chamber (Angelantoni, Italy) with an uncontrolled temperature and humidity curve adjustment program. The temperature in the device is measured with thermocouple sensors. The working temperature range is $-40^{o}C + 180\ ^{o}C$, with a fluctuation of $\pm 0.25°C$-$\pm 0.3°C$ [31].

3.2. Analytical techniques used in the characterization of the studied polymeric materials

3.2.1. Fourier transform infrared spectroscopy (FTIR)

Fourier transform infrared spectroscopy (FTIR) is based on the interaction of IR radiation with matter, providing information about the frequency of radiation at which the substance absorbs electromagnetic radiation and causes vibrations in the molecule.

The FTIR spectra of the samples were drawn using the Tensor 27 FTIR spectrometer (Bruker Optics) in the spectral range 4000-370 cm $^{-1}$. Measurements were made at room temperature, relative humidity 30-40%, using the ATR Platinum module with diamond crystal, and a resolution of 4 cm $^{-1}$, after 64 scans. The signal taken from the detector is converted into a spectrum and processed using an OPUS software [35].

3.2.2. X-ray diffractometry (XRD)

X-ray diffractometry is a technique used to study the crystal structure of materials. The studied sample is irradiated with X-rays, and the resulting diffraction pattern is measured. With the help of this technique, information is obtained about interatomic distances, crystal orientation and other structural details of the studied material [36].

X-ray diffraction measurements were performed with a Rigaku SmartLab rotating anode X-ray diffraction (XRD) equipment equipped with a CuKa1 monochromatic source (λ= 0.15406 nm). To record the diffraction spectra, the "wide angle" configuration was used, in which the position of the source and detector is changed at the same time. The acquisition speed of the spectra was 8 degrees/minute, and the measurement step was set to 0.01 degrees.

3.2.3. UV-VIS spectrophotometry

UV-VIS spectrophotometry is an analytical technique that measures the amount of ultraviolet (UV) and visible (VIS) radiation absorbed by a sample. The UV-VIS spectrophotometer measures the radiation that is absorbed by the sample as a function of wavelength [37].

Cary 5000 UV-Vis-NIR (Agilent Technologies, USA) was used for optical absorption measurements performed at room temperature in the range 1100–200nm.

3.2.4. Scanning Electron Microscopy (SEM)

The technique of scanning electron microscopy (SEM) consists in the analysis of material surfaces with an electron beam down to a nanometric scale [38].

SEM analysis was performed with Nova NanoSEM 630 scanning electron microscope (FEI Company, USA).

3.2.5. Electrical measurements

Volume electrical resistivity is defined as the electrical resistance between opposite faces of a cube of a material with a side of 1 cm. In the present work, the volume resistivity was measured according to ASTM standard 257. The high resistance meter 4339B (Agilent Technologies, USA) with a measurement range up to $4{\times}10^{18}$ Ωcm and the measurement cell 16008B were used.

3.2.6. Dielectric measurements

The dielectric properties of a sample dependent on the operating frequency are measured using dielectric spectroscopy. The measurement principle consists in the interaction of the electric dipole of the sample with the applied electric field. Dielectric spectroscopy measures the impedance of a sample over a frequency range and its energy storage and dissipation properties.

In the present work, the dielectric constant and tangent of the loss angle (dissipation factor) were measured according to the ASTM D150 standard using an Agilent 4294A impedance analyzer (Agilent Technologies, USA) with a measurement range between 40Hz and 110MHz, and a measuring cell 16451B. At the same time, for dielectric measurements of some low-voltage electric cable samples, the device LCR HiTESTER 3532-50 (Hioki, Japan) was used, with a precision of $\pm$ 0.08 % and a response time of 5 ms.

3.2.7. The "extended voltage response" (EVR) method

The extended voltage response (EVR) measurement method is based on the values of the slopes of the decay voltage and the return voltage of the studied dielectric material.

In this analytical technique, the Trek 565 (USA) electrostatic voltmeter is used, having a measuring range of $\pm$1400 V and an accuracy of 1 %.

The electrostatic voltmeter is a voltmeter for measuring surface tension, without the need for electrical charge transfer, without physical contact and implicitly charging the voltage source. In certain situations, using measurement techniques with physical contact and implied transfer of electrostatic charge, there is a risk of distortion of the real value of the voltage or even its disappearance.

3.2.8. Hardness measurements (Shore D)

Shore D hardness testers were performed to measure the penetration depth of degraded and non-degraded samples. The measurement is converted into analog indication on the durometer scale, providing information related to the relative hardness of the studied material. In the present work, the Durometer type D model X.F., according to the ASTM 2240 standard, was used.

Chapter 4
Insulation behavior of subjected low-voltage cables treatment by thermal cycles

This chapter presents the behavior of a low voltage cable with polyvinyl chloride (PVC) insulation subjected to thermal cycles with variable temperatures. An analogy can be made to a situation where a cable is exposed to high temperatures for a period of time and then suddenly experiences a drop in temperature to negative ambient temperature levels.

CYYF 3×1.5 mm2 low voltage cables (Omnicable SRL, Romania) were tested. The component parts of the cable are illustrated in figure 4.1. According to the manufacturer's

information, the conductors are made of copper, the insulation is made of PVC mixture, the filling material mainly contains plasticized PVC granules, the cable jacket is made of PVC mixture.
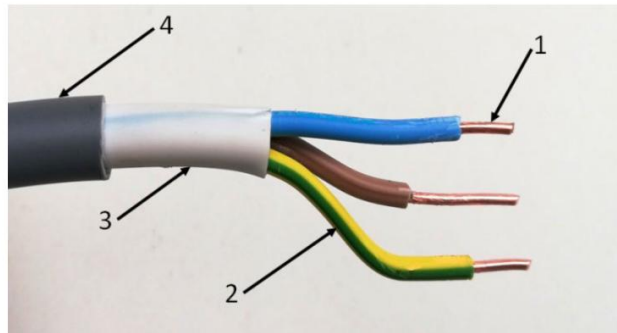
Fig. 4.1. Cable structure: 1 - copper conductor, 2 - conductor insulation, 3 - filling material, 4 - cable jacket. [42].
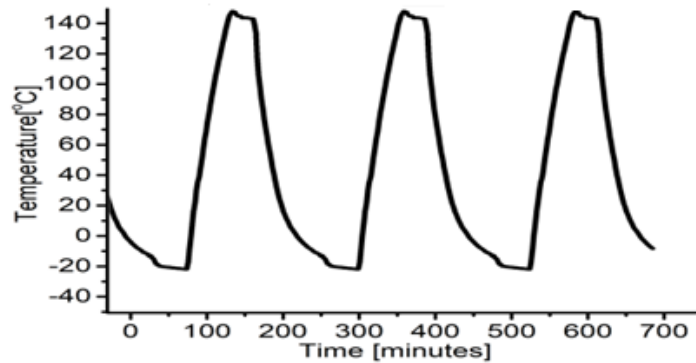
Fig. 4.2. Variation of temperature in the climate chamber as a function of time [42].

The 50 cm long cable samples were placed in the climate chamber with uncontrolled humidity CH 250 TVT.

The maximum positive temperature level was fixed at +140°C, and the lower temperature was set at -20°C, with a temperature change rate of 3°C/min. Figure 4.2 shows the evolution of the temperature in the climatic chamber during the heat treatment.

4.1. Characterization methods

4.1.1. EVR (Extended Voltage Response) method.

In the present study, the variation of the slopes of the decline voltage is analyzed. The source voltage for the charging stage of the EVR test is set to +1000 V and the charging time to 2000 s. The three conductors of the cable are tied together, forming the inner electrode. The outer electrode is made of aluminum foil stretched over the surface of the cable jacket with a length of 44 cm. The outer electrode is grounded to reduce electromagnetic interference.

4.1.2. Dielectric characterization

The loss angle tangent of the studied cable sample was measured with the LCR HiTESTER 3532-50 device (Hioki, Japan), with an accuracy of ± 0.08 % and a response time of 5 ms. The measurements were made in a Faraday cage, made of galvanized steel sheet with the dimensions $80 \times 20 \times 20$ cm^3, so that there are no influences on the results of the measurements, through the effect of electromagnetic waves in the environment.

4.1.3. Mechanical characterization (Shore D)

A durometer type D model X.F. device was used to measure the mechanical parameters, according to the ASTM 2240 standard. The Shore D hardness is a dimensionless value that reflects the hardness of the outer sheath of the cable.

The selection of measurement points was done randomly. Since the geometry of the cable does not conform to the ASTM D2240 standard, which requires a thickness of at least 4 mm for the material, the results of the Shore D mechanical measurements benefit the comparative study.

4.2. Results and Discussion

4.2.1. Results of the "extended voltage response" (EVR) method
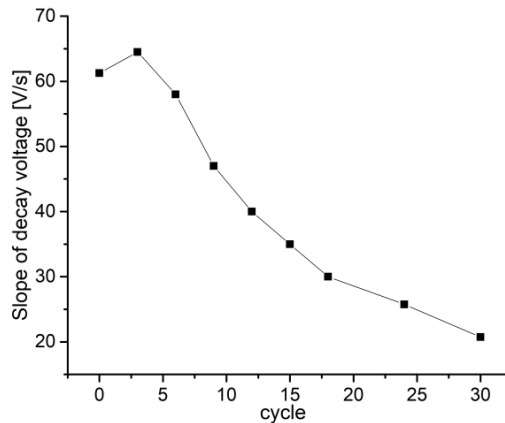
Fig. 4.3. Slope of decay voltages as a function of temperature cycling [42].

According to the results obtained (figure 4.3) after three temperature cycles, there is a redistribution of the plasticizer, its percentage increases significantly, which causes the slope of the decline stress to increase above the initial limit. Then, as thermal cycling progresses, the amount of plasticizer lost increases, causing the slopes of the yield stress to gradually decrease.

4.2.2. Dielectric measurement results
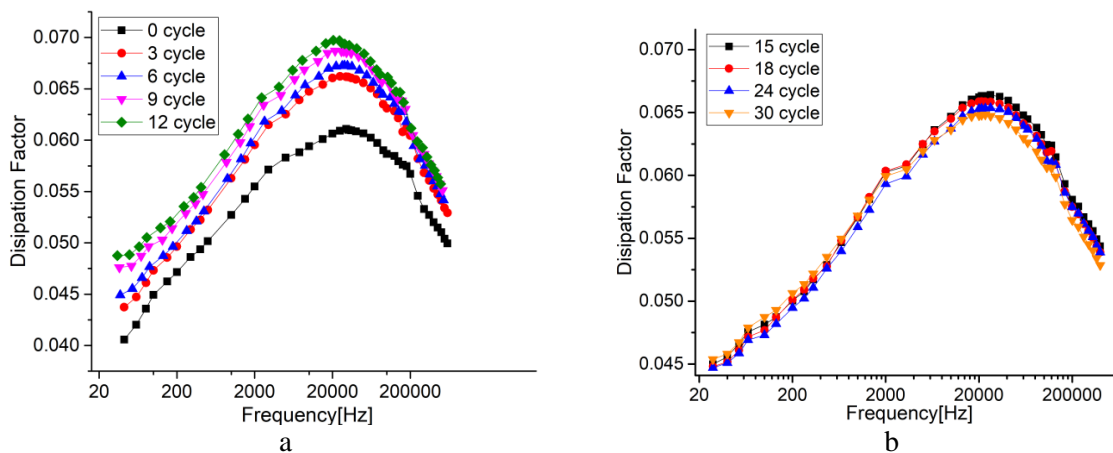
Fig. 4.4. The variation of the dissipation factor measured on the studied frequency range, depending on the temperature cycles: (a) 1 - 12 cycles, (b) 15 - 30 cycles [42].
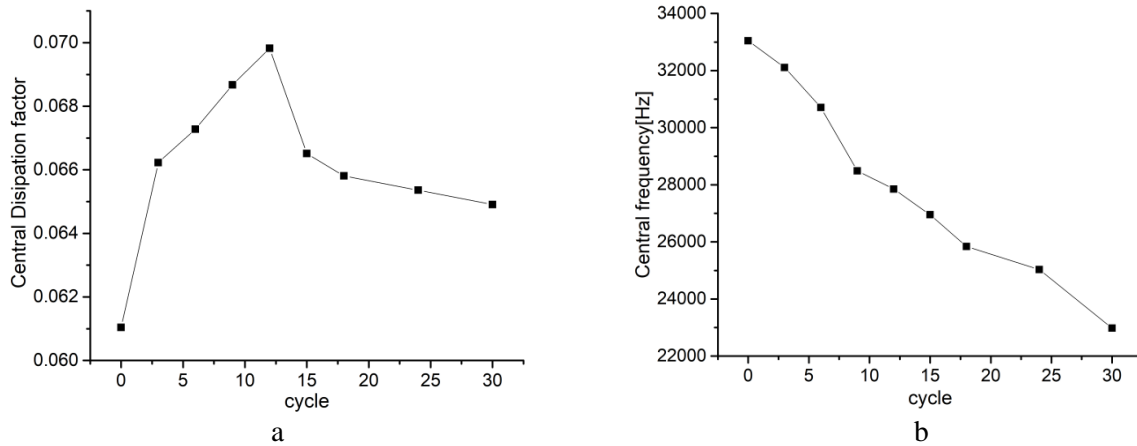
Fig. 4.5 The amplitude of the measured values of the dissipation factor (a) and the frequency corresponding to the measured amplitude of the dissipation factor (b) according to the studied thermal cycles [42].

According to figure 4.4 and 4.5a, the measured values of the dissipation factor, which describe the losses in the dielectric through polarization phenomena, increase up to cycle 12, then have a tendency to decrease with the advancement of the aging process. This phenomenon can be explained by the migration of the plasticizer from the conductor insulation and filler material to the jacket. By the 12th cycle, there is an agglomeration of the plasticizer migrated from the inside to the mantle area, increasing the values of the dissipation factor, because the number of polarizable molecules increases. After the 12th cycle, the loss of plasticizer through the jacket accelerates, which leads to a decrease in the value of the dissipation factor. According to figure 4.5b, the measured central frequency has a decreasing trend during the aging of the cable. The shift to the left of the measured center frequency of the dissipation factor shows that the slower polarization processes become more significant with the aging of the material [53-54].

4.2.3. Mechanical characterization results (Shore D)
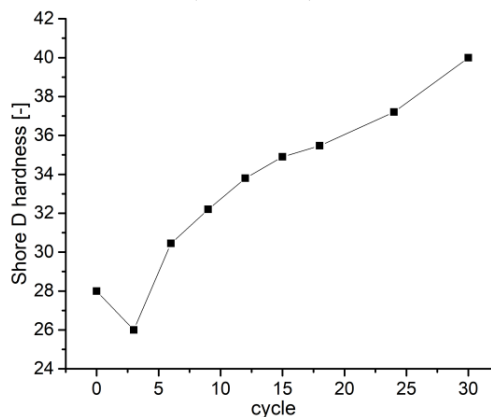
Fig. 4.6. Changes in Shore D hardness of the studied cable samples according to thermal cycles [42].

In figure 4.6, the measurement results are shown after each aging cycle. It can be seen that after the first three heat treatment cycles, the measurements show a sudden softening of the cable jacket. This phenomenon can be explained by the migration of the plasticizer contained in the insulation of the conductors and the filler material to the sheath, causing a sudden softening of the material. Then, as the thermal cycles progress, due to thermal shocks, microcracks appear inside the mantle, increasing the amount of plasticizer released to the

7

outside, while the plasticizer migrating from the inside begins to deplete, thus increasing the hardness of the mantle.

4.3. Conclusions

The measurement results describe the general behavior of the polymer materials in the cable composition and their mode of interaction. The thermal shocks to which the test cable is subjected have the effect of mechanical changes, i.e. microcracks in the cable sheath, which lead to the acceleration of the evaporation of the plasticizer material. The amplitude of the measured dissipation factor and the frequency corresponding to the amplitude of the measured dissipation factor have been shown to be good indicators in assessing the aging condition of the respective cable.

Chapter 5
The study on the gamma ray irradiation of some PVC plates

This chapter presents studies on the changes brought about by gamma radiation on some PVC boards. The respective samples were exposed to gamma radiation, at room temperature at different radiation doses (10, 20, 40, 80) kGy. The changes in the properties of the irradiated PVC plates were studied by the following analytical techniques: UV-Vis spectrophotometry, electrical and dielectric measurements, scanning electron microscopy (SEM).

5.1. Results and discussions
5.1.1. Analysis of color differences
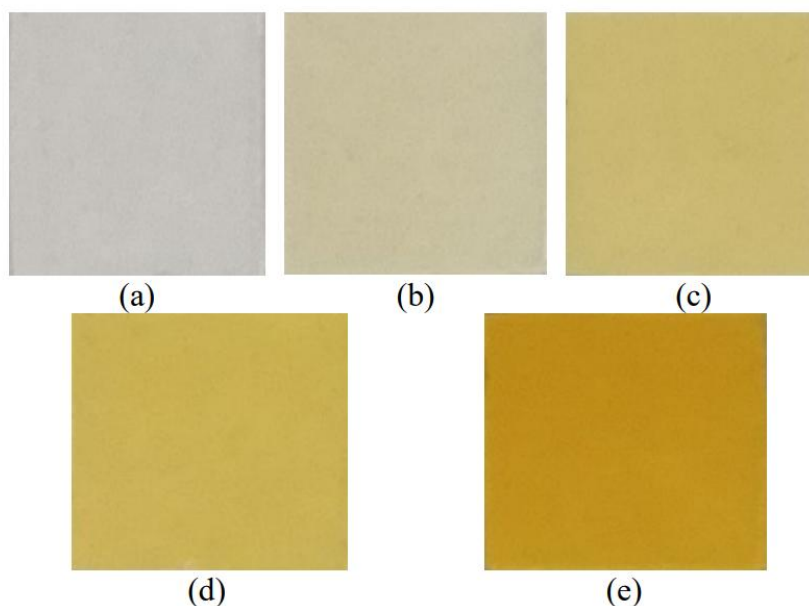
Fig. 5.1. Digital photographs of PVC samples irradiated and irradiated with gamma radiation at different doses: non-irradiated (a), 10 kGy (b), 20 kGy (c), 40 kGy (d) and 80 kGy (e) [39].

PVC irradiated with gamma radiation changes its color (darkens) in proportion to the level of radiation (fig. 5.1). The change in the color of the irradiated samples is due to changes in the polymer structure through the appearance of double bonds along the polymer chain (Zipper effect) [76-78].

5.1.2. Results UV-Vis
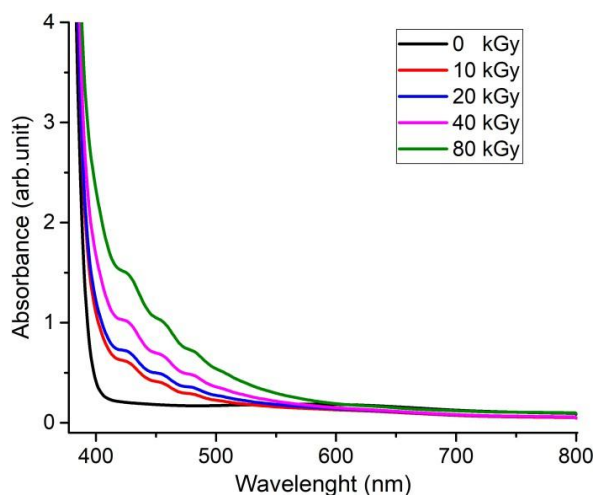
Fig. 5.2. UV-Vis absorbance according to the wavelength of the studied samples [39].

According to figure 5.2, the absorption edge of the UV-Vis spectra, corresponding to the increase in the radiation dose in the samples, moves to the zone of increase in the wavelength. This is due to the newly created chemical configuration, the cross-linking of polymer chains following the action of gamma radiation.

5.1.3. Morphological characterization results (SEM)
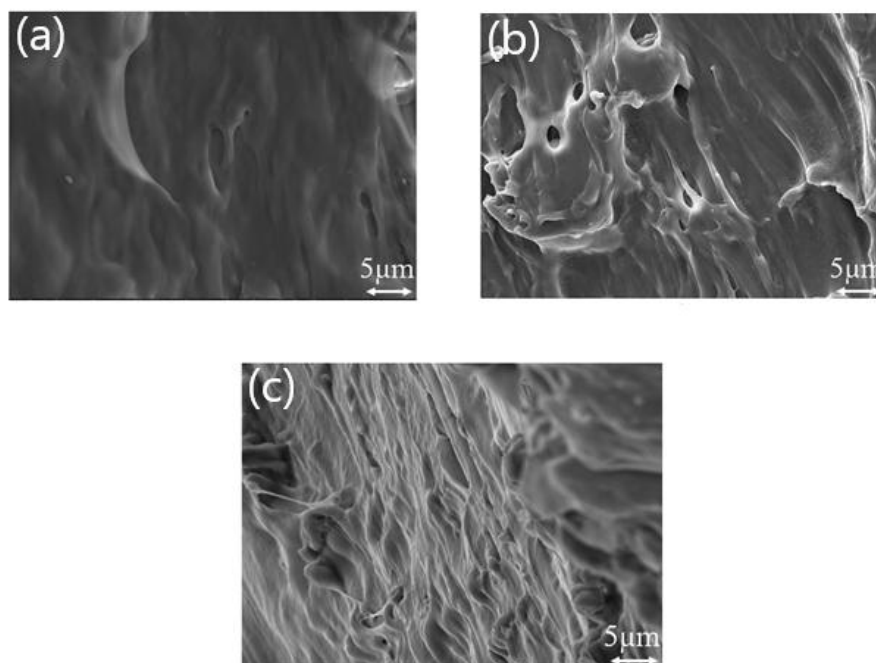
Fig. 5.3. SEM images of fractured PVC sample: (a) non-irradiated, (b) irradiated at 40 kGy, (c) irradiated at 80 kGy at magnification of 5000 × [39].

SEM images, according to Figure 5.3, with a magnification of 5000× show a change in the fracture relief after irradiation at 40 kGy and 80 kGy, compared to the non-irradiated sample. After gamma irradiation, the breaking of the molecular chain occurs, the appearance of free radicals, cross-linking phenomena occur, which leads to a change in morphology.

5.1.4. Dielectric characterization results

(a)   (b)
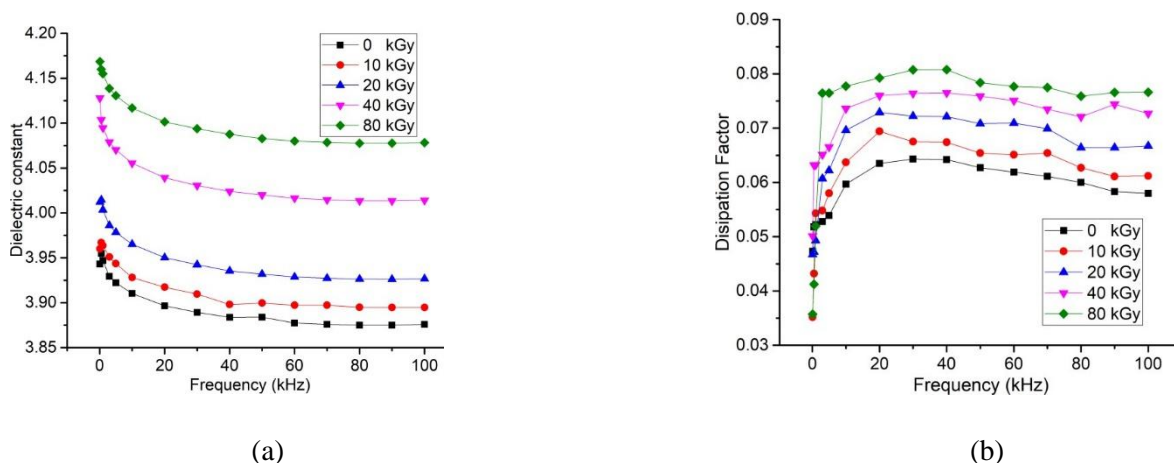
Fig. 5.4. Dielectric constant as a function of frequency for different radiation doses (a), Loss angle tangent as a function of frequency for different radiation doses (b).

According to figure 5.4a, the dielectric constant has higher values in proportion to the irradiation dose. This increase is due to free radicals that form in the polymer structure as a consequence of irradiation. The dielectric constant decreases as the frequency increases, but at high frequencies it remains nearly constant due to the rotational motion of the polymer molecules that do not keep up with the very rapid variation of the electric field.
The tangent of the loss angle increases proportionally with the radiation dose, with a high rate at low frequencies (up to 10 kHz), but after 29 kHz, it shows a slight decrease towards higher ranges (fig.5.4b).

5.1.5. Electrical characterization results
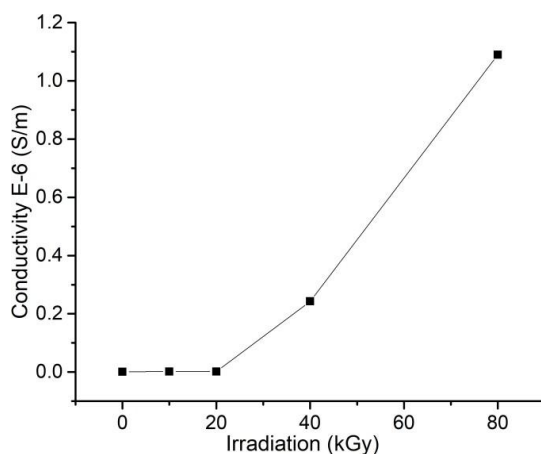
Fig. 5.5. Volume electrical conductivity as a function of radiation dose [39].

Figure 5.5 shows the volume electrical conductivity values measured at different radiation doses at room temperature. The conductivity value increases slightly up to the radiation dose

of 20 kGy. After this value, the conductivity increases steeply due to the more pronounced effect of radiation on the polymer, exponentially increasing the number of free radicals.

5.2. Conclusions

There are changes in the dielectric constant and the tangent of the loss angle, which is the effect of breaking the polymer chain. According to the electrical conductivity analysis, depending on the radiation dose, the phenomenon of breaking the polymer chains occurs, which leads to the appearance of free radicals. The SEM images show a change in the fracture morphology of the gamma-irradiated PVC samples, as a result of the crosslinking of the polymer chains, The value of the radiation absorption rate in the case of UV-Vis measurement increases corresponding to the wavelength greater than 400 nm, due to the crosslinking of the polymer chains. There is also a change in the color of the samples depending on the radiation dose.

Chapter 6
Study of the degradation of epoxy resin subjected to heat treatment by temperature variation

This chapter presents studies on the behavior of epoxy resin samples that were subjected to heat treatment by varying the temperature.

Epoxy resin is a good electrical insulator, has good resistance to corrosion, moisture and chemicals, good mechanical properties and has excellent adhesion to materials. Due to these properties, epoxy resin is mainly used in the electrical, electronic, automotive, aerospace industries.

In the present study, samples of epoxy resin material are subjected to accelerated aging in the form of cycles with temperature variations between +150°C and -20°C.
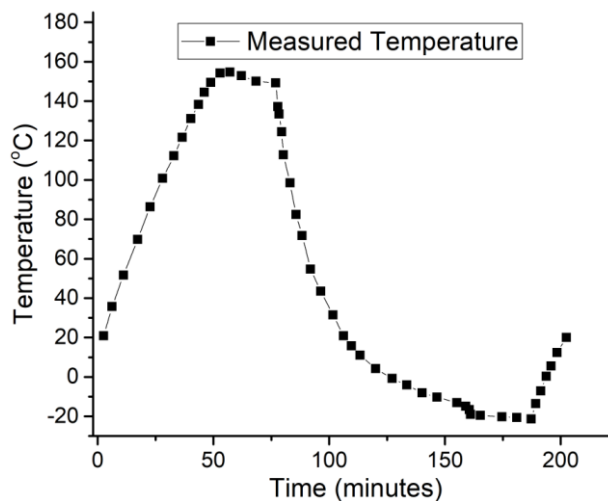
Fig. 6.1. Temperature variation during a single thermal cycle [94].

Figure 6.1 shows the evolution of the temperature measured in the climatic chamber for a thermal cycle that is repeated according to the imposed conditions studied.

6.1. Results and discussion
6.1.1. Color change analysis
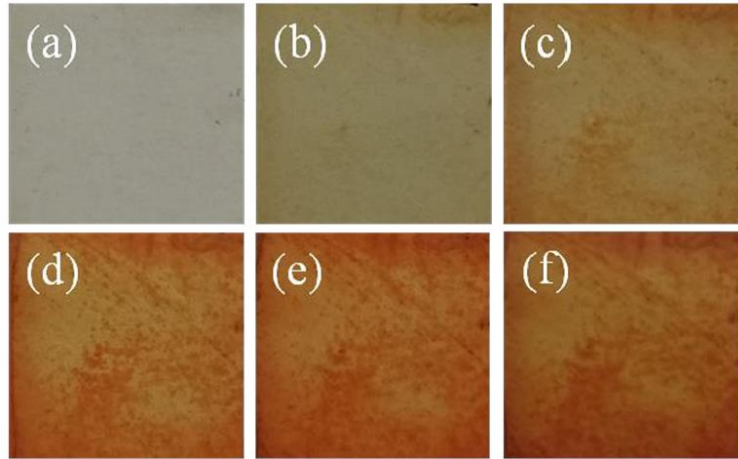
Fig. 6.2. Digital photographs of epoxy resin samples according to the number of temperature cycles imposed: 0 cycles (a), 2 cycles (b), 4 cycles (c), 6 cycles (d), 8 cycles (e), 10 cycles (f) [94]

The heat treatment changes the color of the epoxy resin samples in proportion to the number of cycles, from colorless, yellow, dark yellow and brown (fig. 6.2). This is due to the breaking of polymer chains, oxidation, increase in molecular weight.

6.1.2. Characterization results (UV-Vis)
The absorption spectra corresponding to the wavelength of 300 ÷ 400 nm, obtained by UV-Vis spectroscopy are shown in figure 6.3. The "red-shift" of the maxima at a longer wavelength of the absorption edge of the obtained UV-Vis spectra is due to the appearance of free radicals and cross-linking phenomena in the epoxy resin.
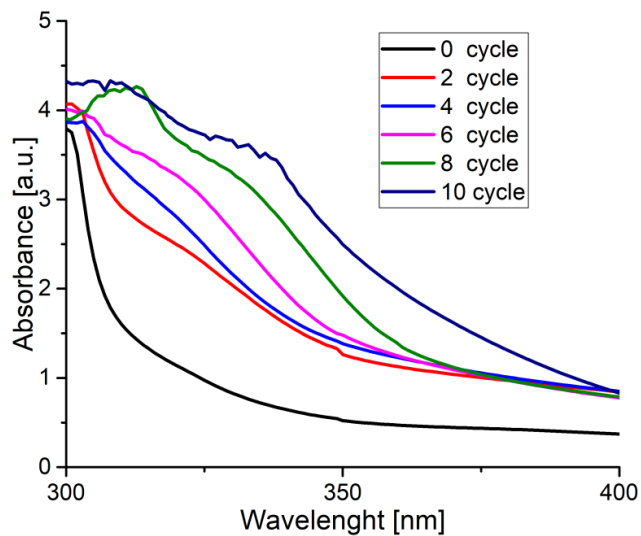
Fig. 6.3 UV-Vis absorption curves of epoxy resin samples after each number of imposed thermal cycles [94].

6.1.3 Spectroscopy results FTIR

(a)   (b)
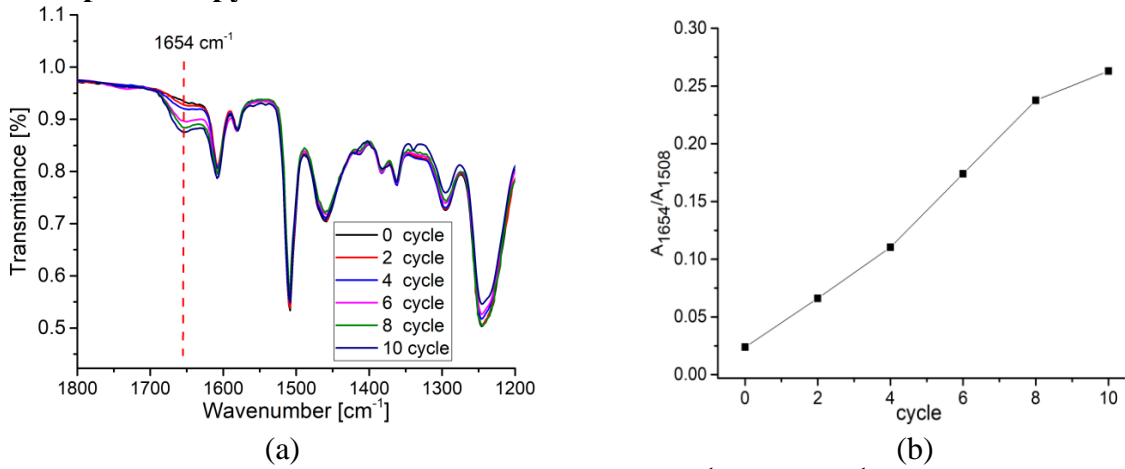
Fig. 6.4 FTIR spectra of epoxy resin in the region 1800 cm^{-1} ÷ 1200 cm^{-1} (a) and the evolution of the carbonyl index (CI) values (b), in the case of each thermal cycle.

For the calculation of the carbonyl index (CI), the area of the absorption band corresponding to the peak of 1654 cm^{-1} was normalized to the area of the absorption band of 1508 cm^{-1} (fig. 6.4a). The results obtained represent an average of 5 measurers. According to figure 6.4b, the carbonyl index (CI) has an upward evolution that can be correlated with the number of heat treatments applied.

6.1.4 Results X-ray diffractometry (XRD)

(a)   (b)
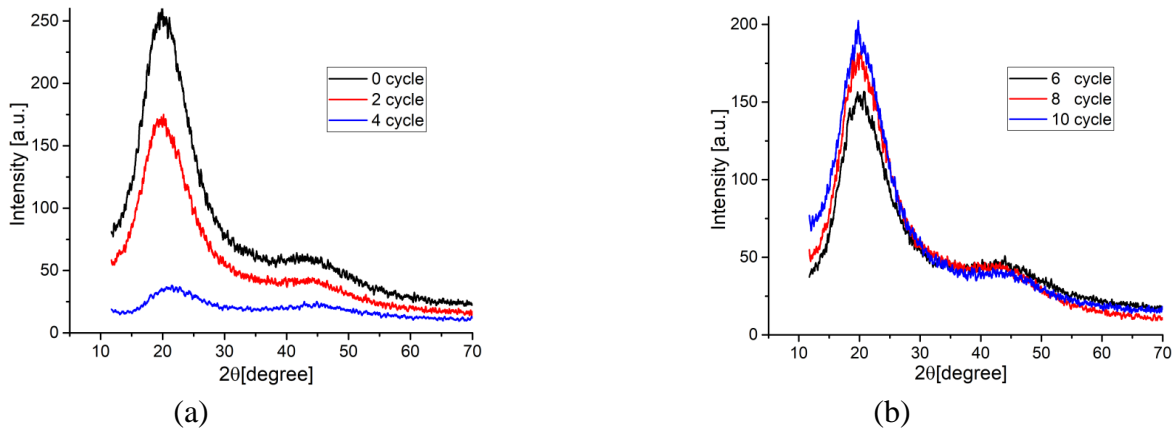
Fig. 6.5. Diffractogram of epoxy resin corresponding to different number of thermal cycles: 0-4 cycles (a), 6-10 cycles (b) [94].

In the first cycles (fig. 6.5a) of the thermal treatment, a process of splitting the polymer chains takes place, resulting in free radicals that combine with oxygen molecules (from diffusion or present in the material), decreasing the degree of crystallinity. In the following cycles (fig. 6.5b), the increase in the number of free radicals produced and the depletion of oxygen molecules cause the free radicals to recombine with each other, overcoming the oxidation process. Crosslinking bridges are created between the polymer molecules. Thus, the polymer chains are arranged in a compact structure, which increases the crystallinity of the epoxy resin [95-96].

6.1.5. Morphological characterization results (SEM)
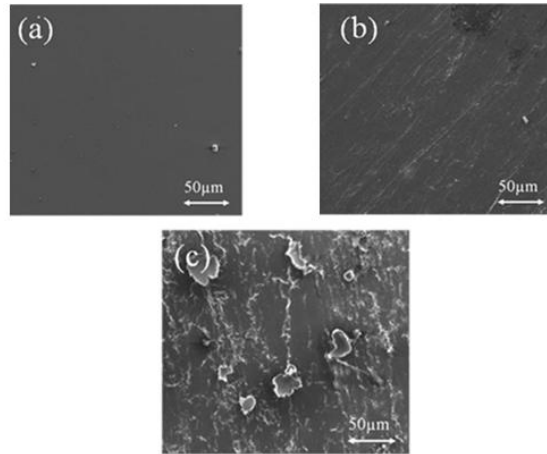
Fig. 6.6. SEM images of the surface morphology of the epoxy resin: non-degraded (a), after 4 thermal cycles (b) and after 10 thermal cycles (c) [94].

According to Figure 6.6, the surface of heat-treated epoxy resin samples has a different morphology compared to non-degraded resin samples. SEM images at 600× magnification show after 4 cycles, a rough surface of the epoxy resin. After 10 cycles, the SEM images show a rougher surface with separated particles and cracks. This fact is due to the difference in expansion and contraction of the surface and interior areas of the polymer during the heat treatment.

6.1.6. Dielectric measurement results

In the first phase of the heat treatment, up to 3 cycles, the dielectric constant tends to increase, due to the increase in the number of dipoles, along with the appearance of free radicals (fig. 6.7a). Up to two cycles, the growth is slower, due to the high electrical viscosity of the material, but with further exposure of the samples to thermal cycles, the electrical viscosity tends to decrease. Therefore, the dipoles under the action of the electric field will rotate more easily, and the material accumulates more energy, the dielectric constant increases. After cycle 4, with the increase in crystallinity, the number of dipoles will decrease, the energy accumulated in the material will be lower, so the dielectric constant tends to decrease. From cycle 6 to cycle 10, the dielectric constant increases, due to the pronounced aging of the material, along with the increase in the number of dipoles.

(a)   (b)
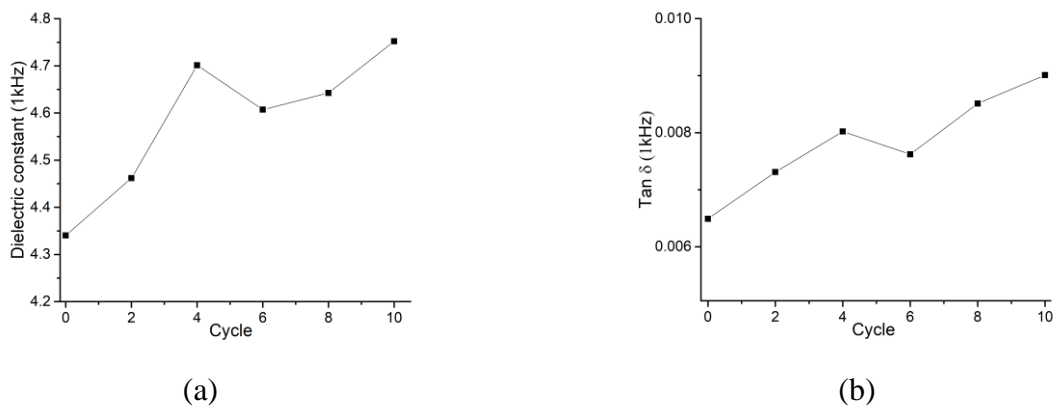
Fig. 6.7. Dielectric constant variation (f=1kHz) (a), Loss angle tangent variation (f=1kHz) (b) during thermal treatments.

The tangent of the loss angle has a tendency to increase up to 4 thermal cycles due to the scission of the polymer chains and implicitly the increase in the concentration of dipoles (figure 6.7b). From 4 to 6 cycles, the tangent of the loss angle decreases due to the decrease in polarization in the context of increased crystallinity due to the combination of free radicals. From 6 to 10 cycles, the loss angle tangent continued its upward trend due to the aging of the epoxy resin, which implies a rapid increase in polymer chain breakage, resulting in a sharp increase in polarization.

6.1.7. Results of electrical measurements (electrical conductivity)
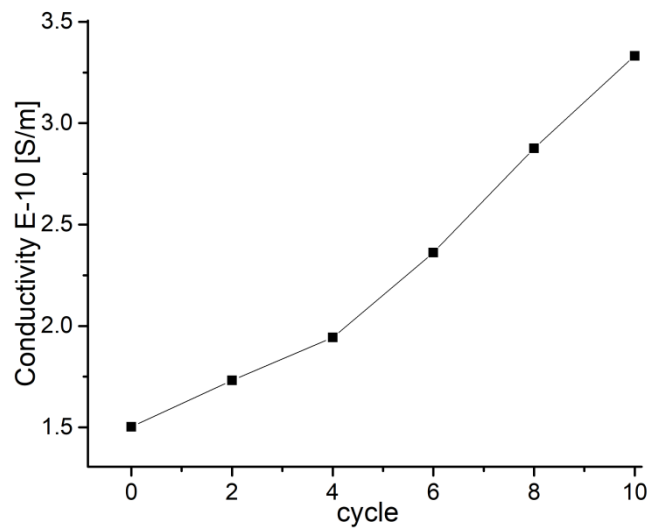
Fig. 6.8. Variation of volume electrical conductivity during heat treatment.

In the case studied, the majority presence of an ionic conductivity is observed. Polymer chain scission during heat treatment causes the number of free radicals to increase proportionally with thermal cycles. In fig. 6.8 the increase in electrical conductivity of the epoxy resin during the thermal cycles can be observed.

6.2. Conclusions

The UV-Vis results show that during the heat treatment, changes occur in the chemical structure of the polymer. FTIR analysis shows the oxidation process by the appearance of carbonyl groups. XRD analysis indicates the variation in crystallinity of the polymer due to oxidation and cross-linking. SEM analysis shows the surface degradation of thermally cycled samples on their surface. Finally, electrical analyzes show an increase in dielectric constant, loss angle tangent, and electrical conductivity during heat treatment. These results show that the epoxy resin degrades under the heat treatments studied and, being an insulating material, can have devastating consequences for the optimal and safe operation of the respective equipment and devices.

Chapter 7

Studies on electromagnetic induction heating of insulated electric conductors

This chapter presents a numerical model that analyzes the heating of a copper electrical conductor with polyvinyl chloride (PVC) insulation.Two cases are considered, namely induction heating and conduction heating. The results of numerical simulations can be used to study the properties of electrical cables, and the presented method is suitable for research in the field of insulation testing. The results of the induction heating simulation are correlated with those obtained from the numerical model of the heating produced by the load or defect electric current passing through the respective conductor leading to its degradation.

7.1. System description

Figure 7.1.a shows the cross section of the induction heating system. The system coil has four turns, having a cylindrical pipe-shaped section through which the coolant (water) passes. The electrical conductor is covered with an insulating layer.

Figure 7.1.b shows the cross-section of the conductor under load, with axial symmetry, surrounded only by the insulation layer.

(a)   (b)
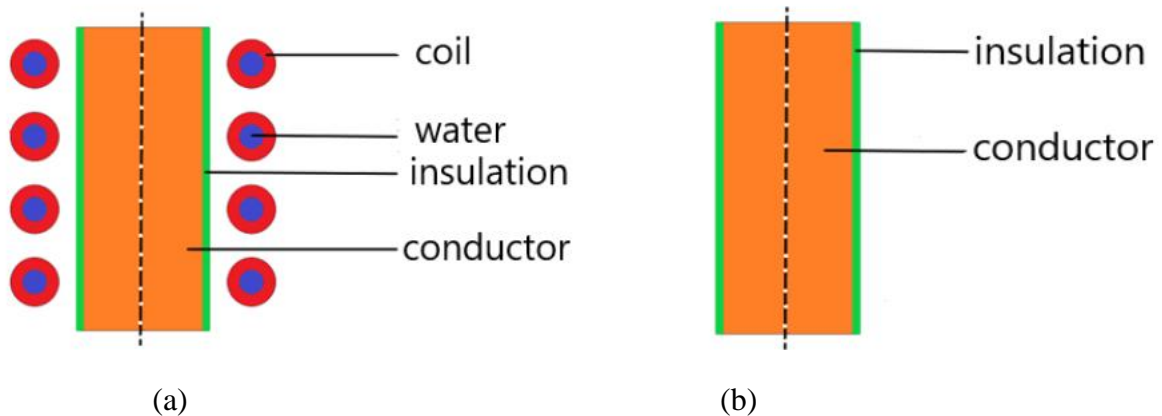
Fig. 7.1. Schematic representation of the two analyzed cases. a – induction heating assembly b – load conductor [109].

7.2. Simulations

Since electrical resistivity, magnetic permeability, thermal conductivity and specific heat with respect to the medium are strongly dependent on temperature, the correct evaluation of the quantities related to the induction heating process requires consideration of the coupling between the electromagnetic field and the thermal field. Also, in this study the coupling between the two electromagnetic and thermal fields is achieved by the fact that the electromagnetic power induced in the studied cable constitutes a force function in the heat transfer equation.

Table 7.1. The physical characteristics and properties of the materials in the studied field

	Copper	PVC	Aer
Electrical conductivity σ (S/m) la 293 ^{o}K	5.8×10^7	-	-
Real part of the complex relative dielectric permittivity at 293 ^{o}K	1	3	1
The imaginary part of the complex relative permittivity at 293oK. The frequency of the electric field is 17 kHz	-	0.085	-
Relative magnetic permeability	1	1	1
Mass density ρ (kg/m^3)	8700	1300	1.3
Thermal conductivity λ (W/(mK)) la 293 ^{o}K	400	0.15	0.025
Specific heat Cp (J/(kgK)) at 293 ^{o}K	385	900	0.001

Table 7.1 shows the properties and physical characteristics of the materials in the studied field

The material of the conductor is made of copper, the length of the conductor is 50mm, the diameter is 20mm, the insulation of the conductor is made of PVC.
The inner diameter of the inductor is 28mm, the outer diameter is 44mm, its height is 50mm, the inductor has 4 turns and has a water-cooling system [109].

Table 7.2. Boundary condition and initial values for the electromagnetic problem

Boundary condition/Initial values	Description
The boundary condition	A = 0
Axis of asymmetry	∂A/∂n = 0
Inductor current (A)	93
The frequency of the inductor current (Hz)	17000

Table 7.2 shows the initial values and boundary conditions for the electromagnetic problem. A voltage of 0.00419 V with a frequency of 50 Hz is imposed at the ends of the conductor under load.

Table 7.3. Initial and boundary condition for heat transfer in the two analyzed situations

Initial temperature T_0 (^{o}K)	293.15
Inductor coolant temperature T (^{o}K)	296
Convection coefficient α (W/m^{2}K)	5
Copper radiation coefficient (β)	0.3
The radiation coefficient PVC (β)	0.9

Table 7.3 shows the initial and boundary conditions for heat transfer in the two analyzed situations.
The inductor is equipped with a water-based cooling system with the equilibrium temperature stabilized at 296 ^{o} K. The simulation time in both cases is set at t = 2500 s.
Figure 7.2 shows the resulting temperature field, in the 2 analysis situations [109].
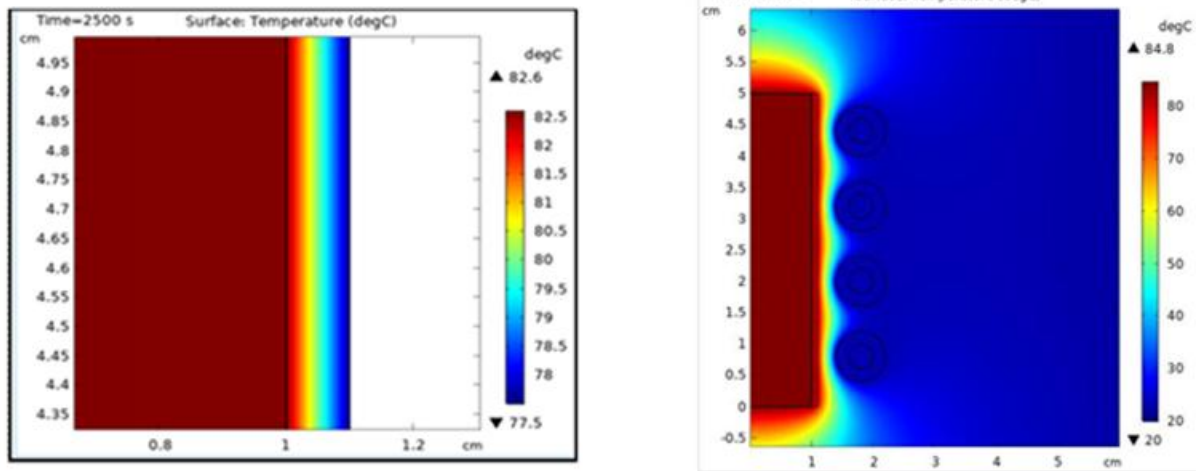
Fig. 7.2. Temperature map for the electric field problem at t = 2500 s (a) Temperature distribution in the conductor – inductor layers at t = 2500 s (b) [109].
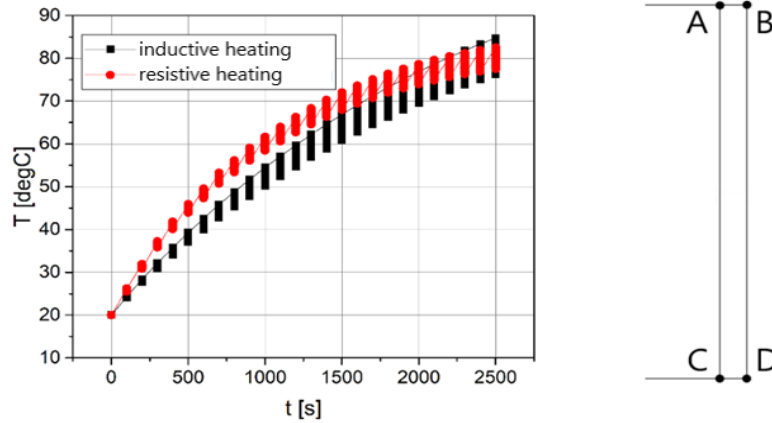
Fig. 7.3. Temperature variation in the ABCD edge in the two analyzed situations [109].
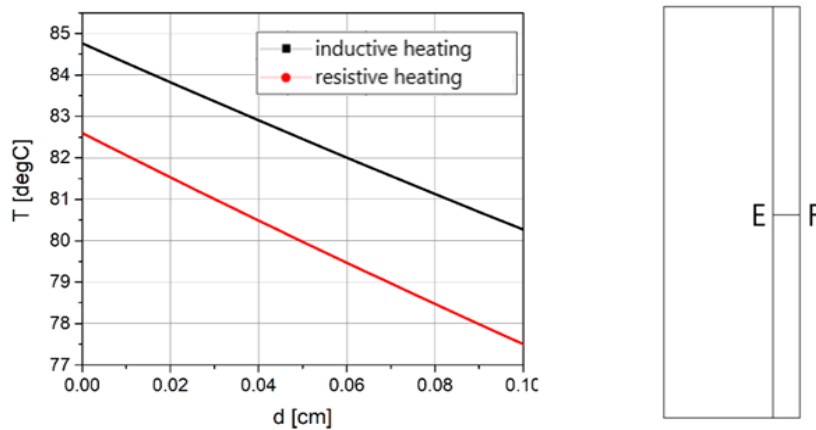
Fig. 7.4. Temperature variation between points E and F in the two analyzed situations [109].
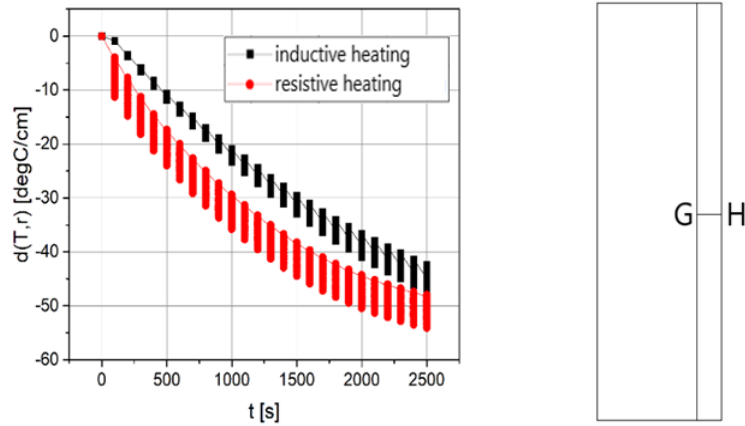
Fig. 7.5. Variation of the temperature gradient between points G and H in the two analyzed situations [109].

A comparison between the temperature variation, in the imposed time interval, obtained in the edge ABCD of the insulating layer is presented in figure 7.3.

Figure 7.4 shows a comparison between the temperature values in the two cases of heating between points E and F. The analysis is carried out in the middle of the conductor through a 1 mm line placed across the entire width of the insulation layer. Fig. 7.5 shows the evolution of the temperature gradient in the two analyzed situations [109].

7.3 Conclusions

Based on the obtained results, it can be seen that the thermal effect of the two methods is almost equivalent.

The proposed electromagnetic induction heating method can be successfully applied to test the thermal degradation of electrical cable insulation, which can replace the conductive heating procedure.

The obtained results can be useful in the case of testing the insulation of electric cables if the thermal degradation of the insulation is done by induction heating.

Chapter 8
General conclusions and original contributions

8.1. General conclusions

In **chapter 4**, the behavior of the PVC insulation of a low-voltage cable subjected to thermal cycles was studied. These cycles are analogous to imminent emergency overloads or certain short-term failures that occur during operation when the cable is exposed to a negative temperature environment. Changes in the structure of the insulation are observed following the tests performed.

In **chapter 5** samples of PVC plates are subjected to gamma radiation at different doses. Measurements performed on non-irradiated and irradiated PVC samples show substantial changes in their structure. As a result of the action of gamma radiation, the breaking of polymer chains, the appearance of free radicals, cross-linking, and changes in molecular weight occur.

The behavior of some epoxy resin samples, studied in chapter 6, subjected to thermal treatment through thermal cycles shows essential changes in the structure, surface morphology, electrical and dielectric changes.

In **chapter 7**, an inductive heating method is proposed in order to test the degradation of electric cables, which can replace the conductive heating method

8.2. Original contributions

The doctoral thesis "Research on the influence of external factors on some polymeric substances" addresses a topic of great interest, which aims at the proper functioning of technical equipment in various fields, having polymeric materials as component parts. The thesis had the following original contributions:

- Study of the degradation of the PVC insulation of a low-voltage cable subjected to thermal cycles with variable temperature, between -20°C and 140°C.

    The study was carried out in the entire volume of the polymeric material, which included: the insulation of the conductors, the filling material and the cable jacket.

    Electrical, dielectric, mechanical tests were carried out in accordance with international standards.

- Degradation study of epoxy resin samples subjected to temperature cycles. The temperature variation was between -20oC and 150oC. To study the characteristics of non-degraded and degraded epoxy resin samples, measurements were made where the following analytical techniques were used: UV-Vis spectrophotometry, FTIR spectroscopy, XRD diffractometry, scanning electron microscopy (SEM).

- Study of electromagnetic induction heating of a PVC insulated electrical conductor. The proposed method can be used to analyze the thermal degradation of electrical cable insulation, which can replace the conductive heating method.

Selective bibliography

[1]   Chris DeArmitt, Applied Plastics Engineering Handbook, Applied Plastics Engineering Handbook, Chapter 26, 2011.

[2]   J. A. Brydson, Plastics material, Biddles Lt4 Guildford and King's Lynn, pp.1-15,1999.

[3]   Dorel, F. Polymer History. Des. Monomers Polym 2008, 11, 1–15. DOI: 10.1163/ 156855508X292383.

[22] Angelika Plota , Anna Masek, Lifetime Prediction Methods for Degradable Polymeric, Materials, 2020.

[23] W Lincoln Hawkins, Polymer Degradation and Stabilization, Springer-Verlag Berlin Heidelberg New York Tokyo, 1984.

[24]   Ghenadii Korotcenkov, Handbook of Humidity Measurement Methods, Materials and Technologies Volume 3: Sensing Materials and Technologie, Taylor & Francis Group, 2020.

[30] Lungulescu, E.M., Fierascu, R.C., Stan, M.S., Fierascu, I. Radoi, E.A. Banciu, C.A. Gabor, R.A. Fistos, T. Marutescu, L. Popa, M. et al., Gamma Radiation-Mediated Synthesis of Antimicrobial Polyurethane Foam/Silver Nanoparticles, Polymers 2024, 16, 1369.

[31 Angelantoni CHALLENGE: Installation, Use And Maintenance Handbook.

[32]   I. Gh. Tanase, "Metode instrumentale de analiza", Vol. II, Metode spectrometrice, Ed. Universitatii Bucuresti (1995).

[33] B. H. Stuart, "Infrared Spectroscopy: Fundamentals and Applications", ANTS (Analytical Techniques in the Sciences) Series, Wiley (2004).

[34] V. Țucureanu, A. Matei, A. M. Avram, „FTIR spectroscopy for carbon family study", Crit. Rev. Anal. Chem., 46(6): 501 - 519 (2016) doi: 10.1080/10408347.2016.1157013.

[35]   J.S. Gaffney, N.A. Marley, and D.E. Jones, Fourier Transform Infrared (FTIR) Spectroscopy, Charact. Mater. (2012) 1104–1135. doi:10.1002/0471266965.

[36] Mario Birkholz, P. F. Fewster, C. Genzel., Thin film analysis by X-ray scattering, Wiley-VCH Verlag GmbH Co., 2005, ISBN-13: 978-3-527-31052-4.

[37] Jian Wu Xianju Zhou, Duo Zhang, Li Li, Sha Jiang, Guotao Xiang, Yongjie Wang, Xiao Tang, Jingfang Li, Zhongmin Cao., Luminescent properties of lanthanide complexes and applications in security anti-counterfeiting and information encryption based on pH response, Volume 257, May 2023, 119686.

[38] J. Goldstein, D. Newbury, D. Joy, C. Lyman, P. Echlin, E. Lifshin, L. Sawyer, and J. Michael, Scanning Electron Microscopy and X-Ray Microanalysis, 3rd edn, Kluwer Academic/Plenum Publishers, New York (2003).

[39] **C.Paun,** D.E.Gavrila, J.Pintea, V.Manescu (Paltanea), V.Stoica, G.Paltanea, I.V.Nemoianu, O.Ionescu, I. Mihalache, O.Brancoveanu, Studies about gamma-ray irradiation of pvc plates used in electric cable insulation, Scientific Bulletin of the Electrical Engineering Faculty – Year 23 No.1 (48) ISSN 2286-2455.

[42] **C.Paun**, D.E.Gavrila, V.Manescu(Paltanea), V.Stoica, G.Paltanea, V.Nemoianu, O.Ionescu, F.Pistritu, Study On The Behavior Of Low-Voltage Cable Insulation Subjected To Thermal Cycle Treatment, Scientific Bulletin of the Electrical Engineering Faculty – Year 23 No.1 (48) ISSN 2286-2455.

[53] Mustafa E, Afia RSA, Nouini O and Tamus ZA. Implementation of non-destructive electrical condition monitoring techniques on low-voltage nuclear cables: I. Irradiation aging of EPR/CSPE cables. Energies 14(16), 5139.

[54] Linde E, Verardi L, Fabiani D, and Gedde UW. Dielectric spectroscopy as a condition monitoring technique for cable insulation based on crosslinked polyethylene. Polym. Test. 2015, 44, 135–142.

[76] Minsker KS, Kolesov SV, Zaikov GE. Degradation and Stabilization of Vinylchloride Based Polymers. Oxford: Pergamon Press, 1988.

[77] Yagoubi N, Baillet A, Legendre B, Rabaron A, and Ferrier D. β-radiation effects on PVC materials: Methodology for studying chemical modifications. J. Appl. Polym. Sci. 1994; 54(8): 1043-1048.

[78] Naimian F, Katbab AA, Nazokdast H. Post-irradiation stability of polyvinyl chloride at sterilizing doses. Rad. Phys. Chem. 1994; 44(6): 567-572.

[94] **Costel PĂUN** , Doina Elena GAVRILĂ , Jana PINTEA , Veronica MANESCU (PALTANEA) , Victor STOICA , Gheorghe PALTANEA , Silviu VULPE , Cosmin ROMANIȚAN , Vasilica ȚUCUREANU , Octavian IONESCU , Iuliana MIHALACHE , Oana BRÎNCOVEANU , Florian PISTRITU, Electrical Behavior Of Epoxy Resin Subjected To Thermal Treatment By Temperature Variation, U.P.B., SCI. BULL SERIES B,VOL 86, ISS.1, 2024, ISSN1454-2331.

[95] E.M. Lungulescu, R. Setnescu, S. Ilie, M. Taborelli, On the use of oxidation induction time as a kinetic parameter for condition monitoring and lifetime evaluation under ionizing radiation environments, in Polymers, **vol. 14**, no. 12, 2022, 2357.

[96] T. Zaharescu, M. Râpă, E.M. Lungulescu, N. Butoi, Filler effect on the degradation of γ-processed PLA/vinyl POSS hybrid, Radiat. Phys. Chem, **vol. 153**, 2018, pp. 188-197.

[109] **Costel Paun** , Doina Elena Gavrilă , Veronica Manescu (Paltanea) , Gheorghe Paltanea, Studies On Electromagnetic Induction Heating Of Electric Conductor Insulation., U.P.B. Sci. Bull., Series C, Vol. 82, Iss. 4, 2020 ISSN 2286-3540.